

## Effect of Friction in Duct Flows

Having described some of the properties and phenomena for steady isentropic duct flows, it is appropriate to digress to described the non-isentropic effects caused by the viscous, frictional effects in ducts since such effects are often of practical importance. Such frictional effects are irreversible, and the flow is therefore non-isentropic. The set of basic equations that are pertinent to any one-dimensional duct flow of a perfect gas through a pipe or duct of constant cross-sectional area, whether that flow is isentropic or non-isentropic, are

- *Continuity:*

$$\rho u A = \text{constant} \quad (\text{Bog1})$$

where, in the present context,  $A$  is constant.

- *Momentum:* See below.

- *Energy:*

$$h^* = c_p T + \frac{u^2}{2} = \text{constant} \quad (\text{Bog2})$$

- *State:*

$$p = \rho \mathcal{R} T \quad (\text{Bog3})$$

and, in differential form, these can be written as

- *Continuity:*

$$\frac{du}{u} + \frac{d\rho}{\rho} = 0 \quad (\text{Bog4})$$

- *Energy:*

$$c_p dT + u du = 0 \quad \text{or} \quad \frac{dT}{T} + (\gamma - 1) M^2 \frac{du}{u} = 0 \quad (\text{Bog5})$$

- *Momentum:*

$$dp + \rho u du + \frac{\rho u^2 f}{2d} dx = 0 \quad (\text{Bog6})$$

where  $f$  is the friction factor of the flow in the duct (assumed known and uniform) and  $d$  is the diameter of the duct (see section (Bfc) for information on the friction factor).

- *State:*

$$\frac{dp}{p} - \frac{d\rho}{\rho} - \frac{dT}{T} = 0 \quad (\text{Bog7})$$

Note that if the friction factor,  $f$ , were set equal to zero these would revert to the set of equations used for steady isentropic duct flow in section (Boe).

Then, using  $M^2 = u^2/c^2 = u^2/\gamma \mathcal{R} T$ , and eliminating  $du$ ,  $dT$ ,  $d\rho$  and  $dp$  from equations (Bog4), (Bog5), (Bog6) and (Bog7) we obtain the relation

$$\frac{f}{d} dx = \left\{ \frac{1 - M^2}{\gamma M^2} \right\} \left\{ 1 + \frac{(\gamma - 1) M^2}{2} \right\}^{-1} \frac{d(M^2)}{M^2} \quad (\text{Bog8})$$

which clearly defines the change in the Mach number in the flow through the duct that results from the effects of friction described by the friction factor,  $f$ . Note that for subsonic flow the Mach number increases with distance along the duct whereas for supersonic flow it decreases. Thus the friction has an effect which is similar to a decreasing cross-sectional area in a flow of varying cross-sectional area. And, moreover, there cannot be any location within the duct where  $M = 1$ . Therefore, we must draw conclusions similar to those we reached in section (Bof). Either the flow in the duct is entirely subsonic (or supersonic) or the flow reaches a Mach number of unity at the end of the duct where, in effect, the flow is choked due to the effect of friction.

Integrating equation (Bog8) (assuming  $f$  remains constant) leads to

$$\frac{f}{d} \int_0^x dx = \frac{fx}{D} = \int_{M_1}^M \left\{ \frac{1 - M^2}{\gamma M^2} \right\} \left\{ 1 + \frac{(\gamma - 1)M^2}{2} \right\}^{-1} \frac{d(M^2)}{M^2} \quad (\text{Bog9})$$

Given  $M_1$  (as well as  $f$ ,  $D$ , and  $\gamma$ ) this equation yields the Mach number,  $M$ , at any location within the duct. Then, with  $M$  determined, the following relations derived from equations (Bog2), (Bog1) and (Bog3) allow the velocity, temperature, density and pressure to be evaluated relative to the hypothetical values at  $M = 1$  (whether or not that point actually occurs in the flow) :

$$\frac{T}{T^*} = 1 + \frac{(\gamma - 1)}{2}(1 - M^2) \quad (\text{Bog10})$$

$$\frac{u}{u^*} = \frac{\rho^*}{\rho} = M \left\{ \frac{T}{T^*} \right\}^{\frac{1}{2}} \quad (\text{Bog11})$$

$$\frac{p}{p^*} = \frac{\rho}{\rho^*} \frac{T}{T^*} \quad (\text{Bog12})$$

The most convenient way to analyze the effects of friction in the steady flow in a duct of uniform cross-sectional area is to consider a hypothetical extension to the pipe to  $x = L^*$  as shown in Figure 1. The flow at the discharge from this extension is assumed to be choked ( $M = 1$ ). Then integrating equation (Bog5)

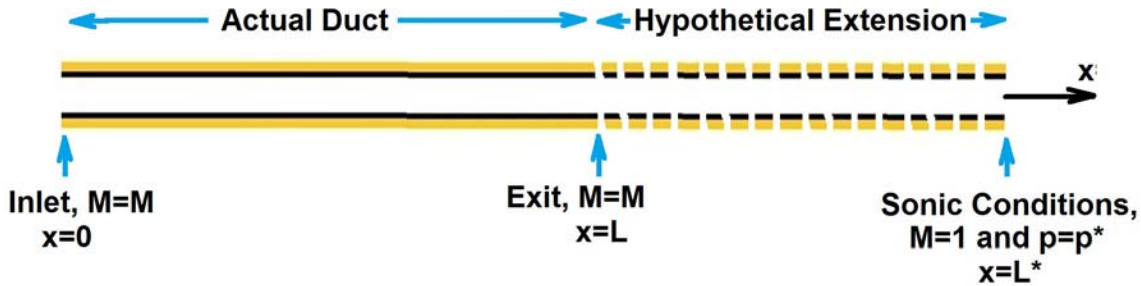


Figure 1: Duct with hypothetical extension to sonic conditions.

(assuming  $f$  remains constant) leads to

$$\frac{f}{d} \int_0^L dx = \frac{fL}{d} = \int_{M_1}^{M_2} \left\{ \frac{1 - M^2}{\gamma M^2} \right\} \left\{ 1 + \frac{(\gamma - 1)M^2}{2} \right\}^{-1} \frac{d(M^2)}{M^2} \quad (\text{Bog13})$$

where  $M_1$  and  $M_2$  are the Mach numbers at inlet to and discharge from the actual duct. Given  $M_1$  (as well as  $f$ ,  $D$ ,  $L$  and  $\gamma$ ) equation (Bog13) provides the value of  $M_2$ . Moreover, since  $M = 1$  at  $x = L^*$  it also follows that

$$\frac{fL^*}{d} = \int_{M_1}^1 \left\{ \frac{1 - M^2}{\gamma M^2} \right\} \left\{ 1 + \frac{(\gamma - 1)M^2}{2} \right\}^{-1} \frac{d(M^2)}{M^2} \quad (\text{Bog14})$$

The most convenient way to solve these relations is to define a function,  $F(M)$ , such that

$$F(M) = \int_M^1 \left\{ \frac{1 - M^2}{\gamma M^2} \right\} \left\{ 1 + \frac{(\gamma - 1)M^2}{2} \right\}^{-1} \frac{d(M^2)}{M^2} \quad (\text{Bog15})$$

It follows that

$$\frac{fL^*}{d} = F(M_1) \quad (\text{Bog16})$$

from which, given  $M_1$ ,  $L^*$  can be determined. Then, knowing  $(L^* - L)$ ,  $M_2$  can be determined from

$$\frac{f(L^* - L)}{d} = F(M_2) \quad (\text{Bog17})$$

Moreover, at any general point in the duct,  $x$ , the Mach number,  $M$ , can be determined from  $f(L^* - x)/d = F(M)$ .

For these purposes  $F(M)$  is tabulated in Figure 3 and plotted in Figure 2. The next step is to determine the velocity ratios,  $u/u^*$ , the temperature ratios,  $T/T^*$ , the density ratios,  $\rho/\rho^*$ , and the pressure ratios,  $p/p^*$  at any point (whether  $x = 0$ ,  $x = L$  or any general location within the duct) using equations (Bog10), (Bog11) and (Bog12) and the Mach number at any of these points. A sample is provided in Figure 2 where the ratios  $u_1/u^*$ ,  $T_1/T^*$ ,  $\rho_1/\rho^*$ , and  $p_1/p^*$  are plotted against the inlet Mach number,  $M_1$ ; this data would allow  $u^*$ ,  $T^*$ ,  $\rho^*$ , and  $p^*$  to be determined given  $u_1$ ,  $T_1$ ,  $\rho_1$ , and  $p_1$ .

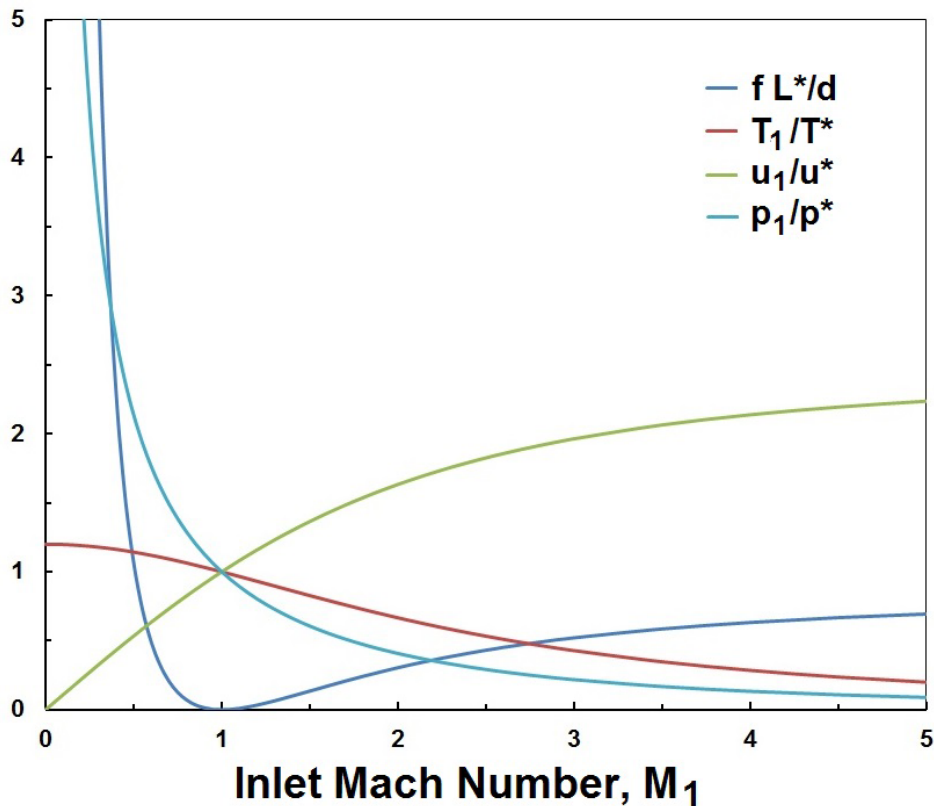


Figure 2: Graphs of  $fL^*/d$ ,  $T_1/T^*$ ,  $u_1/u^*$  and  $p_1/p^*$  against inlet Mach number,  $M_1$ .

$M_1$	$fL^*/d$	$T_1/T^*$	$u_1/u^*$	$\rho_1/\rho^*$	$p_1/p^*$	$M_1$	$fL^*/d$	$T_1/T^*$	$u_1/u^*$	$\rho_1/\rho^*$	$p_1/p^*$
0		1.2	0			1.9	0.274	0.6969	1.5861	0.6305	0.4394
0.05	280.02	1.1994	0.0548	18.262	21.903	1.95	0.29	0.6816	1.6099	0.6211	0.4234
0.1	66.922	1.1976	0.1094	9.1378	10.944	2	0.305	0.6667	1.633	0.6124	0.4082
0.15	27.932	1.1946	0.1639	6.0995	7.2866	2.05	0.32	0.652	1.6553	0.6041	0.3939
0.2	14.533	1.1905	0.2182	4.5826	5.4554	2.1	0.334	0.6376	1.6769	0.5963	0.3802
0.25	8.483	1.1852	0.2722	3.6742	4.3546	2.15	0.348	0.6235	1.6977	0.589	0.3673
0.3	5.299	1.1788	0.3257	3.0702	3.6191	2.2	0.361	0.6098	1.7179	0.5821	0.3549
0.35	3.452	1.1713	0.3788	2.64	3.0922	2.25	0.374	0.5963	1.7374	0.5756	0.3432
0.4	2.308	1.1628	0.4313	2.3184	2.6958	2.3	0.386	0.5831	1.7563	0.5694	0.332
0.45	1.566	1.1533	0.4833	2.0693	2.3865	2.35	0.398	0.5702	1.7745	0.5635	0.3213
0.5	1.069	1.1429	0.5345	1.8708	2.1381	2.4	0.41	0.5576	1.7922	0.558	0.3111
0.55	0.728	1.1315	0.5851	1.7092	1.9341	2.45	0.421	0.5453	1.8092	0.5527	0.3014
0.6	0.491	1.1194	0.6348	1.5753	1.7634	2.5	0.432	0.5333	1.8257	0.5477	0.2921
0.65	0.325	1.1065	0.6837	1.4626	1.6183	2.55	0.442	0.5216	1.8417	0.543	0.2832
0.7	0.208	1.0929	0.7318	1.3665	1.4935	2.6	0.453	0.5102	1.8571	0.5385	0.2747
0.75	0.127	1.0787	0.7789	1.2838	1.3848	2.65	0.462	0.4991	1.8721	0.5342	0.2666
0.8	0.072	1.0638	0.8251	1.2119	1.2893	2.7	0.472	0.4882	1.8865	0.5301	0.2588
0.85	0.036	1.0485	0.8704	1.1489	1.2047	2.75	0.481	0.4776	1.9005	0.5262	0.2513
0.9	0.015	1.0327	0.9146	1.0934	1.1291	2.8	0.49	0.4673	1.914	0.5225	0.2441
0.95	0.003	1.0165	0.9578	1.044	1.0613	2.85	0.498	0.4572	1.9271	0.5189	0.2373
1	0	1	1	1	1	2.9	0.507	0.4474	1.9398	0.5155	0.2307
1.05	0.003	0.9832	1.0411	0.9605	0.9443	2.95	0.514	0.4379	1.9521	0.5123	0.2243
1.1	0.01	0.9662	1.0812	0.9249	0.8936	3	0.522	0.4286	1.964	0.5092	0.2182
1.15	0.021	0.949	1.1203	0.8926	0.8471	3.5	0.586	0.3478	2.0642	0.4845	0.1685
1.2	0.034	0.9317	1.1583	0.8633	0.8044	4	0.633	0.2857	2.1381	0.4677	0.1336
1.25	0.049	0.9143	1.1952	0.8367	0.7649	4.5	0.668	0.2376	2.1936	0.4559	0.1083
1.3	0.065	0.8969	1.2311	0.8123	0.7285	5	0.694	0.2	2.2361	0.4472	0.0894
1.35	0.082	0.8794	1.266	0.7899	0.6947	5.5	0.714	0.1702	2.2691	0.4407	0.075
1.4	0.1	0.8621	1.2999	0.7693	0.6632	6	0.73	0.1463	2.2953	0.4357	0.0638
1.45	0.118	0.8448	1.3327	0.7503	0.6339	6.5	0.743	0.127	2.3163	0.4317	0.0548
1.5	0.136	0.8276	1.3646	0.7328	0.6065	7	0.753	0.1111	2.3333	0.4286	0.0476
1.55	0.154	0.8105	1.3955	0.7166	0.5808	7.5	0.761	0.098	2.3474	0.426	0.0417
1.6	0.172	0.7937	1.4254	0.7016	0.5568	8	0.768	0.087	2.3591	0.4239	0.0369
1.65	0.19	0.777	1.4544	0.6876	0.5342	8.5	0.774	0.0777	2.3689	0.4221	0.0328
1.7	0.208	0.7605	1.4825	0.6745	0.513	9	0.779	0.0698	2.3772	0.4207	0.0293
1.75	0.225	0.7442	1.5097	0.6624	0.4929	9.5	0.783	0.063	2.3843	0.4194	0.0264
1.8	0.242	0.7282	1.536	0.6511	0.4741	10	0.787	0.0571	2.3905	0.4183	0.0239
1.85	0.258	0.7124	1.5614	0.6404	0.4562						

Figure 3: Tabulated values of  $fL^*/d$ ,  $T_1/T^*$ ,  $u_1/u^*$  and  $p_1/p^*$  against inlet Mach number,  $M_1$ .